Strong Localized Perturbations: Theory and Applications

M. J. WARD

Michael J. Ward; Department of Mathematics, University of British Columbia, Vancouver, British Columbia, V6T 1Z2, Canada,

(*July 2015: AARMS Summer School*)

1 An Eigenvalue Optimization Problem and the Mean First Passage Time

We now apply strong localized perturbation theory asymptotics to the problem of determining the mean first passage time (MFPT) for Brownian motion inside a three-dimensional domain with N localized traps. This section is motivated by the recent paper [**4**]. For a fixed trap volume fraction, which spatial arrangement of traps will minimize the average MFPT? Is the effect of fragmentation of the trap set significant? In other words, is there much difference in the MFPT when we replace N small traps by one larger "effective" trap that maintains the volume of the trap set? Such questions are relevant in biological cell signalling when one considers how to model the highly spatially heterogeneous cell cytoplasm.

The mathematical problem is formulated as follows: We consider an optimization problem for the principal eigenvalue of the Laplacian in a bounded three-dimensional domain with a reflecting boundary that is perturbed by the presence of N small traps in the interior of the domain. The perturbed eigenvalue problem is formulated as

$$\Delta u + \lambda u = 0\,, \quad x \in \Omega\backslash\Omega_a\,; \qquad \int_{\Omega\backslash\Omega_a} u^2\,dx = 1\,, \tag{1.1 a}$$

$$\partial_n u = 0\,, \quad x \in \partial\Omega\,, \tag{1.1 b}$$

$$u = 0\,, \quad x \in \partial\Omega_a \equiv \cup_{j=1}^N \partial\Omega_{\varepsilon_j}\,. \tag{1.1 c}$$

Here Ω is the unperturbed domain, $\Omega_a \equiv \cup_{j=1}^N \Omega_{\varepsilon_j}$ is a collection of N small interior traps Ω_{ε_j}, for $j = 1, \ldots, N$, each of 'radius' $\mathcal{O}(\varepsilon) \ll 1$, and $\partial_n u$ is the outward normal derivative of u on $\partial\Omega$. We assume that $\Omega_{\varepsilon_j} \to x_j$ uniformly as $\varepsilon \to 0$, for $j = 1, \ldots, N$, and that the traps are well-separated in the sense that $\mathrm{dist}(x_i, x_j) = \mathcal{O}(1)$ for $i \neq j$ and $\mathrm{dist}(x_j, \partial\Omega) = \mathcal{O}(1)$ for $j = 1, \ldots, N$.

The primary motivation for considering (1.1) is its relationship to determining the mean first passage time (MFPT) for a Brownian particle wandering inside a three-dimensional domain that contains N localized absorbing traps. Denoting the trajectory of the Brownian particle by $X(t)$, the MFPT $v(x)$ is defined as the expectation value of the time τ taken for the Brownian particle to become absorbed somewhere in $\partial\Omega_a$ starting initially from $X(0) = x \in \Omega$, so that $v(x) = E[\tau \,|\, X(0) = x]$. The calculation of $v(x)$ becomes a narrow capture problem in the limit when the volume of the absorbing set $|\partial\Omega_a| = \mathcal{O}(\varepsilon^3)$ is asymptotically small, where $0 < \varepsilon \ll 1$ measures the dimensionless trap radius. Since the MFPT diverges as $\varepsilon \to 0$, the calculation of the MFPT $v(x)$ constitutes a singular perturbation problem. It is well-known (cf. [**6**], [**11**]) that the MFPT $v(x)$ satisfies a Poisson equation with mixed Dirichlet-Neumann boundary

conditions, formulated as

$$\Delta v = -\frac{1}{D}\,, \quad x \in \Omega\backslash\Omega_a\,, \tag{1.2 a}$$

$$\partial_n v = 0\,, \quad x \in \partial\Omega\,; \qquad v = 0\,, \qquad x \in \partial\Omega_a = \cup_{j=1}^{N} \partial\Omega_{\varepsilon_j}\,, \tag{1.2 b}$$

where D is the diffusivity of the underlying Brownian motion. With respect to a uniform distribution of initial points $x \in \Omega$ for the Brownian walk, the average MFPT, denoted by $\bar{v}$, is defined by

$$\bar{v} = \chi \equiv \frac{1}{|\Omega_p|}\int_{\Omega_p} v(x)\,dx\,, \tag{1.3}$$

where $|\Omega_p|$ is the volume of $\Omega_p \equiv \Omega\backslash\Omega_a$.

The mean first passage time v is readily calculated by using the matched asymptotic approach of the previous lecture. Alternatively, v can be calculated by representing it as an eigenfunction expansion in terms of the normalized eigenfunctions ϕ_k and eigenvalues λ_k for $k \geq 0$ of (1.1). In the trap-free domain $\Omega_p = \Omega\backslash\Omega_a$, we readily derive that

$$v = \frac{1}{D}\left[\frac{\phi_0}{\lambda_0}\left(\int_{\Omega_p}\phi_0\,dx\right) + \sum_{k=1}^{\infty}\frac{\phi_k}{\lambda_k}\left(\int_{\Omega_p}\phi_k\,dx\right)\right]. \tag{1.4}$$

For $\varepsilon \to 0$, the principal eigenpair λ_0, ϕ_0, were calculated in the previous lecture, with the result

$$\lambda_0 \sim 4\pi\epsilon|\Omega|^{-1}\sum_{j=1}^{N} C_j\,, \qquad \phi_0 \sim |\Omega|^{-1/2}\,, \quad \text{for} \quad |x - x_j| = \mathcal{O}(1)\,.$$

This shows that $\phi_0\int_{\Omega_p}\phi_0\,dx \sim 1$ and $\lambda_0 = \mathcal{O}(\varepsilon)$ as $\varepsilon \to 0$.

Next, we give a rough estimate of the asymptotic order of the infinite sum in (1.4). This infinite sum does converge for each fixed ε, since $\lambda_k = \mathcal{O}(k^2)$ as $k \to \infty$. However, for each fixed k with $k > 1$, we have that $\lambda_k = \lambda_{k0} + \mathcal{O}(\varepsilon)$ as $\varepsilon \to 0$, where $\lambda_{k0} > 0$ for $k \geq 1$ are the eigenvalues of the Laplacian in the trap-free unit sphere with homogeneous Neumann boundary condition. In addition, for each fixed k with $k \geq 1$, we have that $\int_{\Omega_p}\phi_k\,dx = \mathcal{O}(\varepsilon)$, due to the near orthogonality of ϕ_k and 1 as $\varepsilon \to 0$ when $k \geq 1$. In this way, for $\varepsilon \to 0$, the infinite sum in (1.4) contributes at most an $\mathcal{O}(\varepsilon)$ term, and consequently it can be neglected in comparison with the leading term in (1.4). In particular, one can readily show that the average MFPT $\bar{v}$ is given asymptotically for $\varepsilon \to 0$ in terms of the principal eigenvalue λ_0 by

$$\bar{v} = \chi \sim \frac{1}{D\lambda_0} + \mathcal{O}(\varepsilon)\,. \tag{1.5}$$

This narrow capture problem has wide applications in cellular signal transduction. In particular, in many cases a diffusing molecule must arrive at a localized signaling region within a cell before a signaling cascade can be initiated. Of primary importance then is to determine how quickly such a diffusing molecule can arrive at any one of these localized regions. Our narrow capture problem is closely related to the so-called narrow escape problem, related to the expected time required for a Brownian particle to escape from a confining bounded domain that has N localized windows on an otherwise reflecting boundary. The narrow escape problem has many applications in biophysical modeling (see [**2**], [**6**], [**14**], and the references therein). The narrow escape problem in both two- and three-dimensional confining domains has been studied with a variety of analytical methods in [**6**], [**13**], [**12**], [**7**], [**10**], and [**5**].

We let $\lambda_0(\varepsilon)$ denote the first eigenvalue of (1.1), with corresponding eigenfunction $u_0(x,\varepsilon)$. We have shown that $\lambda_0(\varepsilon) \to 0$ as $\varepsilon \to 0$, and $\lambda_0(\varepsilon) \sim 1/(D\chi)$. One of the main objectives is to derive a two-term asymptotic expansion for $\lambda_0(\varepsilon)$ as $\varepsilon \to 0$. Such a two-term expansion not only provides a more accurate determination, when ε is not too small, of the principal eigenvalue and the corresponding average MFPT, it also provides an explicit formula showing how the locations of the traps within the domain influence these quantities. As explained previously, we emphasize that the leading-order term in the expansion of $\lambda_0(\varepsilon)$ as $\varepsilon \to 0$ is independent of the locations of the traps. By examining the coefficient of the second-order term in the expansion of $\lambda_0(\varepsilon)$ we will formulate a discrete optimization problem for the spatial configuration $\{x_1,\ldots,x_N\}$ of the centers of the N traps of fixed given shapes that maximizes this principal eigenvalue $\lambda_0(\varepsilon)$, and correspondingly minimizes the average MFPT χ.

By using the method of matched asymptotic expansions, we can derive the following two-term result of [**4**]:

Principal Result 2.1: *In the limit of small trap radius, $\varepsilon \to 0$, the principal eigenvalue $\lambda_0(\varepsilon)$ of (1.1) has the two-term asymptotic expansion*

$$\lambda_0(\varepsilon) \sim \frac{4\pi\varepsilon N}{|\Omega|}\bar{C} - \frac{16\pi^2\varepsilon^2}{|\Omega|}p_c(x_1,\ldots,x_N)\,. \tag{1.6 a}$$

Here $\bar{C} \equiv N^{-1}(C_1+\ldots+C_N)$ and $p_c(x_1,\ldots,x_N)$ is the discrete sum defined in terms of the entries $\mathcal{G}_{i,j}$ of the Green's matrix $\mathcal{G}$ of (1.7), as defined below, by

$$p_c(x_1,\ldots,x_N) \equiv c^T\mathcal{G}c = \sum_{i=1}^{N}\sum_{j=1}^{N} C_iC_j\mathcal{G}_{i,j}\,. \tag{1.6 b}$$

The corresponding eigenfunction u is given asymptotically in the outer region $|x-x_j| >> \mathcal{O}(\varepsilon)$ for $j=1,\ldots,N$ by

$$u \sim \frac{1}{|\Omega|^{1/2}} - \frac{4\pi\varepsilon}{|\Omega|^{1/2}}\sum_{j=1}^{N} C_jG(x;x_j) + \mathcal{O}(\varepsilon^2)\,. \tag{1.6 c}$$

For $\varepsilon \ll 1$, the principal eigenvalue $\lambda(\varepsilon)$ is maximized when the trap configuration $\{x_1,\ldots,x_N\}$ is chosen to minimize $p_c(x_1,\ldots,x_N)$. For N identical traps with a common capacitance C, (1.6 a) reduces to

$$\lambda_0(\varepsilon) \sim \frac{4\pi\varepsilon NC}{|\Omega|}\left[1 - \frac{4\pi\varepsilon C}{N}p(x_1,\ldots,x_N)\right], \qquad p(x_1,\ldots,x_N) \equiv \boldsymbol{e}^T\mathcal{G}\boldsymbol{e} = \sum_{i=1}^{N}\sum_{j=1}^{N}\mathcal{G}_{i,j}\,, \tag{1.6 d}$$

where $\boldsymbol{e} = (1,\ldots,1)^T$. Here $G(x;x_j)$ is the Neumann Green's function, satisfying (1.13

In this result, we have defined the capacitance vector c and the symmetric Neumann Green's matrix $\mathcal{G}$ by

$$\mathcal{G} \equiv \begin{pmatrix} R_1 & G_{1,2} & \cdots & G_{1,N} \\ G_{2,1} & \ddots & \ddots & \vdots \\ \vdots & \ddots & \ddots & G_{N-1,N} \\ G_{N,1} & \cdots & G_{N,N-1} & R_N \end{pmatrix}, \qquad c \equiv \begin{pmatrix} C_1 \\ \vdots \\ C_N \end{pmatrix}. \tag{1.7}$$

Here C_j is the capacitance of the j^{th} trap, as defined in the previous lecture, and $G_{i,j} \equiv G(x_i;x_j)$ for $i \neq j$ is the Neumann Green's function of (1.13) with regular part R_j.

At this stage the reader should attempt the following problem:

Problem 1: *Derive Principal Result 2.1 for the special case of N small spherical traps of radii εr_j for $j=1,\ldots,N$,*

by extending the leading-order calculation of the first Neumann eigenvalue of the previous lecture to one higher order. For this case, $C_j = r_j$.

The next result is for the average MFPT.

Principal Result 2.2 *In the limit $\varepsilon \to 0$ of small trap radius, the average mean first passage time $\bar{v}$, based on a uniform distribution of starting points for the Brownian motion, is defined for $\varepsilon \to 0$ by $\bar{v} \sim |\Omega|^{-1} \int_\Omega v\, dx$, and is given explicitly by*

$$\bar{v} \sim \frac{1}{D\lambda_1} + \mathcal{O}(\varepsilon) = \frac{|\Omega|}{4\pi N \bar{C} D \varepsilon}\left[1 + \frac{4\pi\varepsilon}{N\bar{C}} p_c(x_1,\ldots,x_N) + \mathcal{O}(\varepsilon^2)\right]. \tag{1.8}$$

For N identical traps with a common capacitance C, this result reduces to

$$\bar{v} \sim \frac{|\Omega|}{4\pi N \bar{C} D \varepsilon}\left[1 + \frac{4\pi\varepsilon}{N} p(x_1,\ldots,x_N) + \mathcal{O}(\varepsilon^2)\right], \qquad p(x_1,\ldots,x_N) \equiv \sum_{i=1}^{N}\sum_{j=1}^{N} \mathcal{G}_{i,j}\,. \tag{1.9}$$

The derivation of this follows immediately by using the result for $\lambda_0(\varepsilon)$ in Principal Result 2.1 in (1.5) together with (1.5). It also, can be derived from first principles as we now show.

1.1 Derivation of Principal Result 2.2

We now derive (1.8) for the special case of N small spheres, where $\Omega_{\epsilon_j} = \{x \,|\, |x - x_j| = \epsilon r_j\}$ for $j = 1,\ldots,N$. This simplification is not at all essential, but is a little easier to visualize.

As explained above, we cannot simply expand in the outer region $v = v_0 + \epsilon v_1 + \cdots$ since the unperturbed problem

$$\begin{cases} \Delta v_0 = -1/D & \text{for } x \in \Omega \\ \partial_n v_0 = 0 & \text{for } x \in \partial\Omega\,, \end{cases}$$

has no solution. As discussed above, the reason for this is that the associated unperturbed eigenvalue problem has a zero eigenvalue, and the appropriate expansion must be

$$v = \varepsilon^{-1} v_0 + v_1 + \epsilon v_2 + \cdots, \tag{1.10}$$

where v_0 is an unknown constant to be determined.

The problem for v_1 is

$$\begin{cases} \Delta v_1 = -1/D & \text{for } x \in \Omega\backslash\{x_1,\ldots,x_N\} \\ \partial_n v_1 = 0 & \text{for } x \in \partial\Omega \\ v_1 \text{ singular} & \text{as } x \to x_j\,,\ \ j = 1,\ldots,N\,, \end{cases}$$

while v_2 satisfies

$$\begin{cases} \Delta v_2 = 0 & \text{for } x \in \Omega\backslash\{x_1,\ldots,x_N\} \\ \partial_n v_2 = 0 & \text{for } x \in \partial\Omega \\ v_2 \text{ singular} & \text{as } x \to x_j\,,\ \ j = 1,\ldots,N\,. \end{cases}$$

Now in the inner region we let $y = \epsilon^{-1}(x - x_j)$ and $w(y) \equiv v(x_j + \epsilon y)$, and we expand the inner solution as

$$w = \frac{w_0}{\epsilon} + w_1 + \cdots.$$

We obtain, upon using the matching condition $w_0 \to v_0$ as $|y| \to \infty$, that

$$\begin{cases} \Delta_y w_0 = 0 & \text{for } |y| \geq r_j \\ w_0 = 0 & \text{for } |y| = r_j \\ w_0 \to v_0 & \text{as } |y| \to \infty \,. \end{cases}$$

The explicit solution is simply $w_0 = v_0(1 - w_c)$, where $w_c = C_j/|y|$ and $C_j = r_j$. The matching condition for $x \to x_j$ becomes

$$\underbrace{\frac{v_0}{\epsilon} + v_1 + \epsilon v_2 + \cdots}_{x \to x_j} \sim \underbrace{\frac{w_0}{\epsilon} + w_1 + \cdots}_{y \to \infty} = \frac{v_0}{\epsilon}\left(1 - \frac{C_j}{|x - x_j|}\epsilon\right) + w_1 + \cdots \,.$$

Therefore, we obtain

$$v_1 \to -\frac{v_0 C_j}{|x - x_j|}\,, \quad \text{as} \quad x \to x_j \,.$$

The problem for v_1 is simply

$$\begin{cases} \Delta v_1 = -1/D & \text{for } x \in \Omega \backslash \{x_1, \ldots, x_N\} \\ \partial_n v_1 = 0 & \text{for } x \in \partial\Omega \\ v_1 \sim -\frac{v_0 C_j}{|x - x_j|} & \text{as } x \to x_j \,,\ j = 1, \ldots, N \,, \end{cases}$$

which is equivalent to

$$\begin{cases} \Delta v_1 = -1/D + 4\pi v_0 \sum_{j=1}^{N} C_j \delta(x - x_j) & \text{for } x \in \Omega \\ \partial_n v_1 = 0 & \text{for } x \in \partial\Omega \,. \end{cases} \tag{1.11}$$

Upon using the divergence theorem, we obtain that

$$-\frac{|\Omega|}{D} + 4\pi v_0 \sum_{j=1}^{N} C_j = 0 \,. \tag{1.12}$$

This yields the leading-order outer solution as

$$v \sim \frac{v_0}{\epsilon}\,, \qquad \text{where} \quad v_0 = \frac{|\Omega|}{4\pi D \sum_{j=1}^{N} C_j}\,,$$

where $C_j = r_j$.

Now we proceed to one higher order in the asymptotic construction. To do so, we must solve for v_1 explicitly. This is done by introducing the Neumann Green's function $G(x; x_j)$ defined uniquely by the solution to

$$\Delta G = \frac{1}{|\Omega|} - \delta(x - x_j)\,, \quad x \in \Omega \,, \tag{1.13 a}$$

$$\partial_n G = 0\,, \quad x \in \partial\Omega \,, \tag{1.13 b}$$

$$\int_\Omega G \, dx = 0 \,. \tag{1.13 c}$$

We notice that $G(x; x_j)$ exists since $\int_\Omega \left(\frac{1}{|\Omega|} - \delta(x - x_j)\right) dx = 0$, and the condition $\int_\Omega G \, dx = 0$ specifies G uniquely, as it eliminates an otherwise arbitrary additive constant for G. As $x \to x_j$ we obtain

$$G(x; x_j) \sim \frac{1}{4\pi|x - x_j|} + R_j + o(1)\,, \quad \text{as} \quad x \to x_j \,, \tag{1.13 d}$$

where R_j, which depends on x_j and Ω, is called the regular part of G.

We now claim that the solution to (1.11) is

$$v_1 = -4\pi v_0 \sum_{i=1}^{N} C_i G(x;x_i) + \chi\,, \tag{1.14}$$

where χ is an unknown constant to be determined. We verify that

$$\begin{aligned}\Delta v_1 &= -4\pi v_0 \sum_{i=1}^{N} C_i \Delta G(x;x_i)\,,\\ &= -\frac{4\pi v_0}{|\Omega|}\sum_{i=1}^{N} C_i + 4\pi v_0 \sum_{j=1}^{N} C_j \delta(x-x_j)\\ &= -\frac{1}{D} + 4\pi v_0 \sum_{j=1}^{N} C_j \delta(x-x_j)\,.\end{aligned}$$

where the last line follows by using (1.12). In addition, we observe from (1.14) that since $\int_\Omega G(x;x_j) = 0$, the unknown constant χ has the interpretation that it is the spatial average of v_1, i.e. $\bar{v}_1 = \chi = \frac{1}{|\Omega|}\int_\Omega v_1\,dx$. This is the key quantity we wish to calculate since it will determine the second term in the expansion of the average MFPT.

Now we expand the solution in (1.14) as $x \to x_j$ for each $j = 1,\dots,N$ to obtain

$$v_1 \sim B_j + \chi - \frac{\mu C_j}{|x-x_j|}\,, \qquad \text{as} \qquad x \to x_j\,,$$

where B_j is defined by

$$B_j = -4\pi u_0 \left(C_j R_j + \sum_{i\neq j}^{N} C_i G(x_j;x_i)\right). \tag{1.15}$$

Upon returning to the matching condition

$$\frac{v_0}{\epsilon} + v_1 + \epsilon v_2 + \cdots \sim \frac{w_0}{\epsilon} + w_1 + \cdots\,,$$

we write this condition out in more detail to get

$$\frac{v_0}{\epsilon} + B_j + \chi - \frac{v_0 C_j}{|x-x_j|} + \epsilon v_2 \sim \frac{\mu}{\epsilon}\left(1 - \frac{C_j\epsilon}{|x-x_j|}\right) + w_1\,. \tag{1.16}$$

This implies that for each $j = 1,\dots,N$, w_1 must satisfy

$$\begin{cases} \Delta_y w_1 = 0 & \text{for } |y| \geq r_j\\ w_1 = 0 & \text{for } |y| = r_j\\ w_1 \sim B_j + \chi & \text{as } |y| \to \infty\,. \end{cases}$$

The solution is given explicitly by

$$w_1 = (B_j + \chi)\left(1 - \frac{C_j}{|y|}\right)\,.$$

where $C_j = r_j$ is the capacitance of the j-th trap.

Upon substituting this back into the matching condition (1.16), we obtain that v_2 must satisfy

$$\begin{cases} \Delta v_2 = 0 & \text{for } x \in \Omega\backslash\{x_1,\dots,x_N\}\\ \partial_n v_2 = 0 & \text{for } x \in \partial\Omega\\ v_2 \sim -(B_j+\chi)\frac{C_j}{|x-x_j|} & \text{as } x \to x_j \quad j = 1,\dots,N\,. \end{cases}$$

Therefore, we can write the problem for v_2 as

$$\Delta v_2 = 4\pi \sum_{j=1}^{N} (B_j + \chi) C_j \delta(x - x_j) \qquad x \in \Omega\,; \qquad \partial_n v_2 = 0\,, \quad \text{on} \quad \partial\Omega\,.$$

Finally, we determine χ by the divergence theorem. We calculate that the problem for v_2 has a solution iff

$$\sum_{j=1}^{N} (B_j + \chi) C_j = 0\,,$$

so that

$$\chi = -\frac{\sum_{j=1}^{N} B_j C_j}{\sum_{j=1}^{N} C_j}\,. \tag{1.17}$$

where B_j is defined in (1.15). In this way, we obtain the two-term expansion

$$\bar{v} \sim \frac{v_0}{\epsilon} + \chi\,.$$

By introducing a vector notation and the Green's matrix, this result is equivalent to that in Principal Result 2.2.

1.2 Applications of Principal Result 2.2

We now minimize the coefficient of the second-order term in the asymptotic expansion of $\bar{v}$ of Principal Result 2.2 for the special case when Ω is a sphere of radius one that contains N small identically-shaped traps of a common "radius" ε. To do so, we require the Neumann Green's function of (1.13) for the unit sphere as given explicitly by (see Appendix A of [**4**])

$$G(x;\xi) = \frac{1}{4\pi|x-\xi|} + \frac{1}{4\pi|x||x'-\xi|} + \frac{1}{4\pi}\log\left(\frac{2}{1-|x||\xi|\cos\theta+|x||x'-\xi|}\right) + \frac{1}{6|\Omega|}\left(|x|^2+|\xi|^2\right) - \frac{7}{10\pi}\,, \tag{1.18 a}$$

where $|\Omega| = 4\pi/3$. Here $x^{'} = x/|x|^2$ is the image point to x outside the unit sphere, and θ is the angle between ξ and x, i.e. $\cos\theta = x\cdot\xi/|x||\xi|$, where $\cdot$ denotes the dot product.

To calculate $R(\xi)$ from (1.18 *a*) we take the limit of $G(x,\xi)$ as $x \to \xi$ and extract the nonsingular part of the resulting expression. Setting $x = \xi$ and $\theta = 0$ in (1.18 *a*), we obtain $|x' - \xi| = -|\xi| + 1/|\xi|$, so that

$$R(\xi) = \frac{1}{4\pi\left(1-|\xi|^2\right)} + \frac{1}{4\pi}\log\left(\frac{1}{1-|\xi|^2}\right) + \frac{|\xi|^2}{4\pi} - \frac{7}{10\pi}\,. \tag{1.18 b}$$

Next, we compute optimal spatial arrangements $\{x_1,\ldots,x_N\}$ of $N \geq 2$ identically shaped traps inside the unit sphere that minimizes $p(x_1,\ldots,x_N)$ in (1.9). To simplify the computation, we will minimize the function $\mathcal{H}_{\rm ball}$ defined in terms of p of (1.6 *d*) by

$$\mathcal{H}_{\rm ball} \equiv \sum_{i=1}^{N}\sum_{j=1}^{N} \widetilde{\mathcal{G}}_{i,j} = \sum_{i=1}^{N}\sum_{j=1}^{N} \left((1-\delta_{ij})\widetilde{G}_{ij} + \delta_{ij}\widetilde{R}_{ii}\right)\,, \qquad p(x_1,\ldots,x_N) = \frac{\mathcal{H}_{\rm ball}}{4\pi} - \frac{7N^2}{10\pi}\,, \tag{1.19}$$

where $\delta_{ij} = 0$ if $i \neq j$ and $\delta_{jj} = 1$. Here we have defined $\widetilde{\mathcal{G}}_{i,j}$, $\widetilde{G}_{i,j}$ and $\widetilde{R}_{j,j}$ by $\widetilde{\mathcal{G}}_{i,j} = 4\pi(\mathcal{G}_{i,j} - B)$, $\widetilde{G}_{i,j} \equiv 4\pi(G_{i,j} - B)$, and $\widetilde{R}_{j,j} \equiv 4\pi(R_{j,j} - B)$, where $B = -7/(10\pi)$ and $G_{i,j}$ and $R_{j,j}$ are obtained from (1.18).

Various numerical methods for global optimization are available, including

N	$\mathcal{H}_{\rm ball}^{(a)}$	Spherical radii $r_1 = ... = r_N$	$\mathcal{H}_{\rm ball}^{(b)}$	Spherical radii $r_2 = ... = r_N$ $(r_1 = 0)$
2	**7.2763**	0.429	9.0316	0.563
3	**18.5047**	0.516	20.3664	0.601
4	**34.5635**	0.564	36.8817	0.626
5	**56.2187**	0.595	58.1823	0.645
6	**82.6490**	0.618	85.0825	0.659
7	**115.016**	0.639	116.718	0.671
8	**152.349**	0.648	154.311	0.680
9	**195.131**	0.659	196.843	0.688
10	**243.373**	0.668	244.824	0.694
11	**297.282**	0.676	297.283	0.700
12	**355.920**	0.683	357.371	0.705
13	**420.950**	0.689	421.186	0.710
14	**491.011**	0.694	491.415	0.713
15	**566.649**	0.698	566.664	0.717
16	647.738	0.702	**647.489**	0.720
17	734.344	0.706	**733.765**	0.722
18	826.459	0.709	**825.556**	0.725
19	924.360	0.712	**922.855**	0.727
20	1027.379	0.715	**1025.94**	0.729

Table 1. Numerically computed minimal values of the discrete energy functions $\mathcal{H}_{\rm ball}^{(a)}$ and $\mathcal{H}_{\rm ball}^{(b)}$ for the optimal arrangement of N-traps within a unit sphere, as computed using the DSO method. The numerically computed minimum value of $\mathcal{H}_{\rm ball}$ in (1.19) is shown in bold face.

(1) *The Extended Cutting Angle method (ECAM).* This deterministic global optimization technique is applicable to Lipschitz functions. Within the algorithm, a sequence of piecewise linear lower approximations to the objective function is constructed. The sequence of the corresponding solutions to these relaxed problems converges to the global minimum of the objective function (cf. [**1**]).

(2) *Dynamical Systems Based Optimization (DSO).* A dynamical system is constructed, using a number of sampled values of the objective function to introduce "forces". The evolution of such a system yields a descent trajectory converging to lower values of the objective function. The algorithm continues sampling the domain until it converges to a stationary point (cf. [**9**]).

Our computational results given below for the minimization of (1.19) were obtained by using the open software library `GANSO` (cf. [**8**]), where both the ECAM and DSO methods are implemented.

The optimal trap pattern when N is small, consisting of N traps on one inner sphere, is found to switch to an optimal pattern with $N-1$ traps on an inner sphere and one at the origin as N is increased. We compare the minimal values of the discrete energy $\mathcal{H}_{\rm ball}$ in (1.19) for the case (a) when all traps are forced to lie on one sphere ($\mathcal{H}_{\rm ball}^{(a)}$), and in the case (b) when one trap remains at the origin ($r_1 = 0$), while the remaining traps lie on one inner sphere ($\mathcal{H}_{\rm ball}^{(b)}$). These optimal energy values and the corresponding inner sphere radii, computed with the DSO method, are

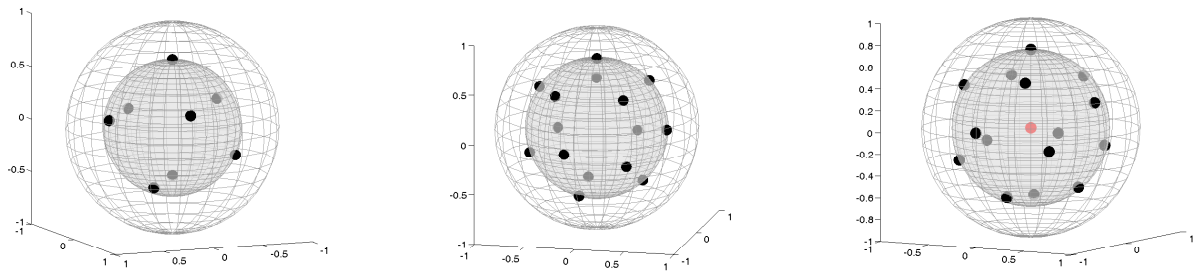

(a) $N = 8$ (b) $N = 15$ (c) $N = 16$

Figure 1. Numerically computed optimal spatial arrangements of traps inside a unit sphere. For $N = 8$ and $N = 15$ all traps are on an interior sphere. For $N = 16$ there is one trap at the origin, while 15 traps are on an interior sphere.

given in Table 1. For each N with $2 \leq N \leq 15$, our results show that the optimal configuration has N traps located *on a single inner sphere* within the unit sphere. The case $N = 16$ is the smallest value of N that deviates from this rule. In particular, for $16 \leq N \leq 20$, there is one trap located at the origin ($r_1 = 0$), while the remaining $N-1$ traps are located on one interior sphere so that $r_2 =, \ldots, = r_N$.

We remark that the numerically computed minima of the energy function $\mathcal{H}_{\rm ball}$ in (1.19) were computed directly using the ECAM and DSO methods, and the results obtained were found to coincide with the results shown in Table 1 computed from the restricted optimization problem associated with $\mathcal{H}^{(a)}_{\rm ball}$ for $2 \leq N \leq 15$ and with $\mathcal{H}^{(b)}_{\rm ball}$ for $N = 16, 17, 18$. In Fig. 1 we show the numerically computed optimal spatial arrangements of traps for $N = 8, 15, 16$. We also remark that the numerical optimization problem becomes increasingly difficult to solve as N increases, due to the occurrence of many local minima.

For the special case of N traps with a common capacitance $C = C_j$ for $j = 1, \ldots, N$ inside the unit sphere Ω, then $\bar{v}$ in (1.8) becomes

$$\bar{v} \sim \frac{|\Omega|}{D}\left[\frac{1}{4\pi\varepsilon NC} + \frac{1}{N^2}p(x_1,\ldots,x_N)\right], \qquad p(x_1,\ldots,x_N) = \sum_{i=1}^{N}\sum_{j=1}^{N}\mathcal{G}_{ij} = \frac{\mathcal{H}_{\rm ball}}{4\pi} - \frac{7N^2}{10\pi}, \tag{1.20}$$

where $\mathcal{H}_{\rm ball}$ is the discrete energy defined in (1.19). Next, we use (1.20) to illustrate the effect on $\bar{v}$ of trap clustering. For $N = 20$ optimally placed spherical traps of a common radius ε, we set $C = 1$ and use the last entry for $\mathcal{H}_{\rm ball}$ in Table 1 for $N = 20$ to evaluate p in (1.20). In contrast, suppose that there are $N = 10$ clusters of two touching spheres of a common radius ε inside the unit sphere. Assume that the clusters are optimally located within the unit sphere. For this arrangement, we set $N = 10$ in (1.20), and use the capacitance $C = 2\log 2$ of two touching spheres, together with optimal value for $\mathcal{H}_{\rm ball}$ given in Table 1 for $N = 10$. In this way, we obtain

$$\bar{v} \sim \frac{|\Omega|}{D}\left(\frac{1}{80\pi\varepsilon} - 0.01871\right), \quad \text{(no trap clustering)}; \qquad \bar{v} \sim \frac{|\Omega|}{D}\left(\frac{1}{80\pi\varepsilon\log 2} - 0.02915\right), \quad \text{(trap clustering)}. \tag{1.21}$$

Therefore, to leading order, this case of trap clustering increases the average MFPT by a factor of $1/\log 2$ for $\varepsilon \ll 1$.

Principal Result 2.2 can be used to show the influence of the number N of distinct subregions comprising the trap set. In this way, we study the effect of fragmentation of the trap set. We consider N spherical traps of a common radius

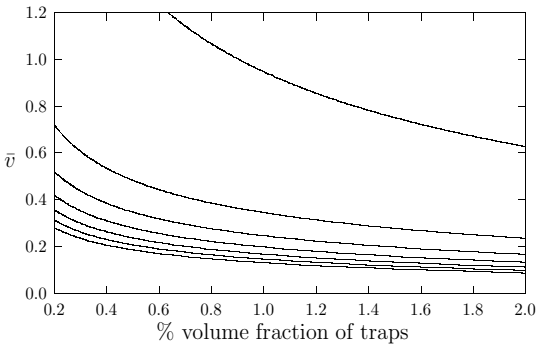

Figure 2. The average MFPT $\bar{v}$ in (1.8) with $D = 1$ versus the percentage trap volume fraction $100f = 100\varepsilon^3 N$ for the optimal arrangement of N identical traps of a common radius ε in the unit sphere. Plot for $N = 1, 5, 8, 11, 14, 17, 20$ (top to bottom curves).

ε inside the unit sphere. We denote the percentage trap volume fraction by $100f$, where $f = 4\pi\varepsilon^3 N/(3|\Omega|) = \varepsilon^3 N$. In Fig. 2 we plot $\bar{v}$, given in (1.20) with $C = 1$, versus the trap volume percentage fraction $100f$ corresponding to the optimal arrangement of $N = 5, 8, 11, 14, 17, 20$ traps, as computed from the global optimization routine discussed above (see Table 1). In this figure we also plot $\bar{v}$ for a single large trap with the same trap volume fraction. We conclude that even when f is small, the effect of fragmentation of the trap set is rather significant.

At this stage, we list a few open problems:

Open Problems:

(1) Provide reliable computations of the global minimum of the discrete energy $\mathcal{H}_{ball}$ for N large. Determine a scaling law for it that is valid as $N \to \infty$, which would yield a scaling law for the average MFPT $\bar{v}$.

(2) Does the optimal arrangement of traps for large N exhibit some underlying hexahedron-type symmetry. Can the limiting asymptotics be predicted by the dilute fraction limit of homogenization theory?

(3) Calculate the modified Green's function and its regular part numerically for other 3-D domains to determine the eigenvalue asymptotics as well as a scaling law for the optimal average MFPT. How can one reliably compute the Neumann Green's function in (1.13) for an arbitrary domain given that one must impose the constraint $\int_\Omega G\, dx = 0$.

2 Splitting Probabilities

Next, we use the method of matched asymptotic expansions to calculate the splitting probabilities of [**3**]. The splitting probability $u(x)$ is defined as the probability of reaching a specific target trap Ω_{ε_1} from the initial source point $x \in \Omega\backslash\Omega_a$, before reaching any of the other surrounding traps Ω_{ε_j} for $j = 2, \ldots, N$. It is well-known that u satisfies (cf. [**3**])

$$\Delta u = 0\,, \quad x \in \Omega\backslash\Omega_a \equiv \cup_{j=1}^N \Omega_{\varepsilon_j}\,; \qquad \partial_n u = 0\,, \quad x \in \partial\Omega\,, \tag{2.1 a}$$

$$u = 1\,, \quad x \in \partial\Omega_{\varepsilon_1}\,; \qquad u = 0\,, \quad x \in \cup_{j=2}^N \partial\Omega_{\varepsilon_j}\,. \tag{2.1 b}$$

By developing a two-term matched asymptotic expansion the following result can be obtained:

Principal Result 2.3: *In the limit $\varepsilon \to 0$ of small trap radius, the splitting probability u, satisfying (2.1), is given asymptotically in the outer region $|x - x_j| \gg \mathcal{O}(\varepsilon)$ for $j = 1, \ldots, N$ by*

$$u \sim \frac{C_1}{N\bar{C}} + 4\pi\varepsilon C_1 \left[G(x; x_1) - \frac{1}{N\bar{C}} \sum_{j=1}^{N} C_j G(x; x_j) \right] + \varepsilon\chi_1 + \mathcal{O}(\varepsilon^2)\,, \tag{2.2 a}$$

where χ_1 is given by

$$\chi_1 = -\frac{4\pi C_1}{N\bar{C}} \left[(\mathcal{G}c)_1 - \frac{1}{N\bar{C}} c^T \mathcal{G} c \right]. \tag{2.2 b}$$

Here $\mathcal{G}$ is the Green's matrix of (1.7), $c = (C_1, \ldots, C_N)^T$, and $(\mathcal{G}c)_1$ is the first component of $\mathcal{G}c$. The averaged splitting probability $\bar{u} \equiv |\Omega|^{-1} \int_\Omega u\, dx$, which assumes a uniform distribution of starting points $x \in \Omega$, is

$$\bar{u} \sim \frac{C_1}{N\bar{C}} + \varepsilon\chi_1 + \mathcal{O}(\varepsilon^2)\,. \tag{2.2 c}$$

2.1 Derivation of Principal Result 2.3

We now only derive the leading-order term in this result. For a derivation that includes the second-order term see §3 of [**4**].

In the outer region, we expand u as

$$u = u_0 + \varepsilon u_1 + \varepsilon^2 u_2 + \cdots\,. \tag{2.3}$$

Here u_0 is an unknown constant, and u_k for $k = 1, 2$ satisfies

$$\Delta u_k = 0\,, \quad x \in \Omega \backslash \{x_1, \ldots, x_N\}\,; \qquad \partial_n u_k = 0\,, \quad x \in \partial\Omega\,, \tag{2.4}$$

with certain singularity conditions as $x \to x_j$ for $j = 1, \ldots, N$ determined upon matching to the inner solution.

In the inner region near the j^{th} trap, we expand the inner solution $w(y) \equiv u(x_j + \varepsilon y)$, with $y \equiv \varepsilon^{-1}(x - x_j)$, as

$$w = w_0 + \varepsilon w_1 + \cdots\,. \tag{2.5}$$

Upon substituting (2.5) into (2.1 *a*) and (2.1 *b*), we obtain that w_0 and w_1 satisfy

$$\Delta_y w_0 = 0\,, \quad y \notin \Omega_j\,; \qquad w_0 = \delta_{j1}\,, \quad y \in \partial\Omega_j\,, \tag{2.6 a}$$

$$\Delta_y w_1 = 0\,, \quad y \notin \Omega_j\,; \qquad w_1 = 0\,, \quad y \in \partial\Omega_j\,. \tag{2.6 b}$$

Here $\Omega_j = \varepsilon^{-1}\Omega_{\varepsilon_j}$, and δ_{j1} is Kronecker's symbol. The far-field boundary conditions for w_0 and w_1 are determined by the matching condition as $x \to x_j$ between the the inner and outer expansions (2.5) and (2.3), respectively, written as

$$u_0 + \varepsilon u_1 + \varepsilon^2 u_2 + \cdots \sim w_0 + \varepsilon w_1 + \cdots\,. \tag{2.7}$$

The first matching condition is that $w_0 \sim u_0$ as $|y| \to \infty$, where u_0 is an unknown constant. Then, the solution

for w_0 in the $j^{\rm th}$ inner region is given by

$$w_0 = u_0 + (\delta_{j1} - u_0)\, w_c(y)\,, \tag{2.8}$$

where $\delta j1 = 1$ if $j = 1$ and $\delta_{j1} = 0$ for $j \neq 1$. Here w_c is the solution to the capacitance problem for the j-th trap

$$\begin{cases} \Delta_y w_c = 0 & \text{for } y \notin \Omega_j \\ w_c = 1 & \text{for } y \in \partial\Omega_j \\ w_c \to 0 & \text{as } |y| \to \infty\,. \end{cases} \tag{2.9 a}$$

which has the far-field asymptotics

$$w_c \sim \frac{C_j}{|y|} + \frac{\mathbf{p_j}\cdot y}{|y|^3} + \mathcal{O}(|y|^{-3})\,, \quad \text{as } |y| \to \infty\,, \tag{2.9 b}$$

where C_j is the capacitance and $\mathbf{p}_j$ the dipole moment of Ω_j. Upon, using this far-field asymptotic behavior w_c, we obtain that

$$w_0 \sim u_0 + (\delta_{j1} - u_0)\left(\frac{C_j}{|y|} + \frac{P_j\cdot y}{|y|^3}\right), \quad \text{as } \ y \to \infty\,. \tag{2.10}$$

From (2.10) and (2.7), we conclude that u_1 satisfies (2.4) with singular behavior $u_1 \sim (\delta_{j1} - u_0)\, C_j/|x - x_j|$ as $x \to x_j$ for $j = 1, \ldots, N$. Therefore, in terms of the Dirac distribution, u_1 satisfies

$$\Delta u_1 = -4\pi \sum_{j=1}^{N} (\delta_{j1} - u_0)\, C_j \delta(x - x_j)\,, \quad x \in \Omega\,; \qquad \partial_n u_1 = 0\,, \quad x \in \partial\Omega\,. \tag{2.11}$$

The solvability condition for u_1, obtained by the divergence theorem, determines the unknown constant u_0 as

$$u_0 = \frac{C_1}{N\bar{C}}\,, \qquad \bar{C} \equiv \frac{1}{N}\left(C_1 + \cdots C_N\right)\,. \tag{2.12}$$

This completes the derivation of the first term in the main result of Principal Result 2.3.

2.2 Applications and Illustration of Principal Result 2.3

From (2.2 a) we observe that $u \sim C_1/(N\bar{C})$, so that there is no leading-order effect on the splitting probability u of either the location of the source, the target, or the surrounding traps. If $C_j = 1$ for $j = 1, \ldots, N$, then $u \sim 1/N$. Therefore, for this equal-capacitance case, then to leading-order in ε it is equally likely to reach any one of the N possible traps. If the target at x_1 has a larger capacitance C_1 than those of the other traps at x_j for $j = 2, \ldots, N$, then the leading order theory predicts that $u > 1/N$. The formulae for the capacitances in the Table given in the last lecture can be used to calculate the leading order term for u for different shapes of either the target or surrounding traps.

Next, we use (2.2) to illustrate the more interesting effect on u of the relative locations of the source, target, and surrounding traps. In the two examples below, Ω is taken to be the unit sphere, for which the Green's function and its regular part, required in (2.2), are given analytically in (1.18 a) and (1.18 b), respectively.

We first consider the two-trap case $N = 2$. Then, (2.2) is readily reduced to

$$u \sim \frac{C_1}{C_1 + C_2} + 4\pi\varepsilon C_1 \left(\frac{C_2}{C_1 + C_2}\left(G_1 - G_2\right) - \frac{1}{(C_1 + C_2)^2}\left[C_2\left(C_1 R_1 - C_2 R_2\right) + C_2\left(C_2 - C_1\right) G_{12}\right]\right). \tag{2.13}$$

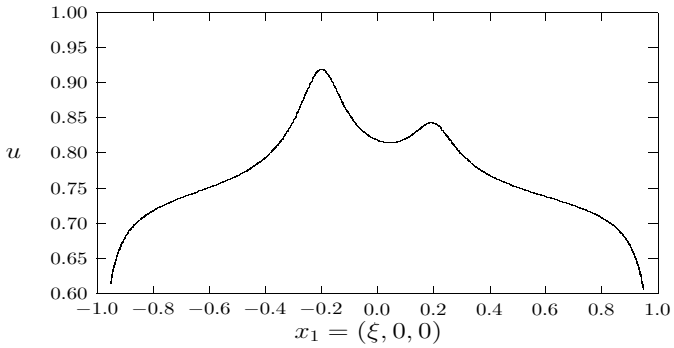

Figure 3. Left figure: u versus the location $x_1 = (\xi, 0, 0)$ of the centre of a target sphere of radius 1.5ε. The other trap centred at $x_2 = (0.2, 0.08, 0.0)$ is a sphere of radius 0.5ε. Here $\varepsilon = 0.04$ and the source is at $x = (-0.2, 0.08, 0)$.

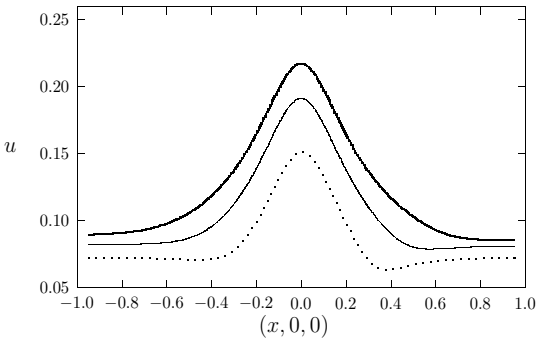

Figure 4. Plot of the splitting probability u versus the location $x = (x, 0, 0)$ of the source for a target trap centred at $x_1 = (0, 0, 0.2)$ surrounded by nine traps centred at optimally spaced points on an inner sphere that is concentric with the unit sphere. The inner sphere has radius $r_s = 0.7$ (heavy solid curve), $r_s = 0.5$ (solid curve), or $r_s = 0.35$ (dashed curve). The target and surrounding traps are spheres of a common radius $\varepsilon = 0.04$ so that $C_j = 1$ for $j = 1, \ldots, 10$. Right figure: same spatial configuration of traps with $\varepsilon = 0.04$ except that the target sphere has twice the capacitance of the surrounding traps, i.e. $C_1 = 2$ and $C_j = 1$ for $j = 2, \ldots, 10$.

Here we have defined $G_1 \equiv G_1(x; x_1)$, $G_2 \equiv G_2(x; x_1)$, $G_{12} \equiv G_1(x_1; x_2)$, $R_1 \equiv R(x_1)$, and $R_2 \equiv R(x_2)$. We first consider the specific example in [**3**] corresponding to a target centred at a variable point $x_1 = (\xi, 0, 0)$, a trap centred at $x_2 = (0.2, 0.08, 0.0)$, and a fixed source location at $x = (-0.2, 0.08, 0)$. The target is a sphere of radius 1.5ε, while the other trap is a sphere of radius 0.5ε, where $\varepsilon = 0.04$. Thus, $C_1 = 1.5$ and $C_2 = 0.5$. The probability u of first reaching the target trap at $x_1 = (\xi, 0, 0)$, with $-1 < \xi < 1$, is shown in Fig. 3, and agrees with Fig. 12(b) of [**3**]. The notable qualitative feature in Fig. 3 of u having two local maxima is discussed in [**3**]. The leading order theory predicts that $u \sim C_1/(C_1 + C_2) = 3/4$, but the higher-order in ε influence of the spatial configuration of target, trap, and source, as seen in Fig. 3, is clearly significant even at $\varepsilon = 0.04$.

Next, we consider a nontrivial example of (2.2) for $N = 10$ traps that has an interesting qualitative interpretation. We take a target trap centred near the origin at $x_1 = (0, 0, 0.2)$ and surround it with 9 traps with centres optimally spaced on an inner sphere that is concentric with the unit disk Ω (the specific location of these points is given in §3 of [**4**]). The inner sphere is taken to have radius $r_s = 0.7$, $r_s = 0.5$, or $r_s = 0.35$. The target and surrounding traps are

spheres with a common radius $\varepsilon = 0.04$, so that $C_j = 1$ for $j = 1, \ldots, 10$. In Fig. 4 we plot u, computed from (2.2), for a source position on the x-axis at location $(x, 0, 0)$ with $-1 < x < 1$. For these parameter values, the leading order theory predicts that $u \sim 0.1$. From Fig. 4 we observe a clear screening effect. When the source is outside the inner sphere, which effectively acts as a "wall" of traps, it is difficult to reach the target sphere centred at $(0, 0, 0.2)$. Therefore, when the source is outside the inner sphere we would expect $u < 0.1$. This is clearly observed in Fig. 4. However, we would expect that u increases considerably when the source crosses inside the inner sphere, as the target sphere is then well-isolated from the surrounding traps and is in closer proximity to the source. If the inner sphere has a smaller radius, such as $r_s = 0.35$, then the target sphere is not as isolated from the surrounding traps as when $r_s = 0.7$. Correspondingly, the peak in u is not as pronounced near the origin when $r_s = 0.35$ as it is for larger values of r_s. This is precisely what is observed in Fig. 4. The local minimum in u in the dashed curve of Fig. 4 for a source point at $(x, 0, 0) \approx (0.35, 0, 0)$ is due to a nearby trap on the inner sphere centred at $x_2 \approx (0.327, 0.0, 0.125)$. This nearby trap significantly lowers the probability that the target near the origin will be reached first.

There are many other qualitatively interesting applications of Principal Result 3.2 for different arrangements of a target and surrounding traps. However, we emphasize that (2.2) applies only in the outer region $|x - x_j| \gg \mathcal{O}(\varepsilon)$ and for $|x_i - x_j| \gg \mathcal{O}(\varepsilon)$. Thus, the source and traps must be well-separated, and no two traps can be closely spaced by $\mathcal{O}(\varepsilon)$. For two closely-spaced, but non-overlapping, spherical traps of the same radius, one can use our previous results for the capacitance of the two-sphere cluster and then modify (2.2) accordingly.

References

[1] G. Beliakov, *The Cutting Angle Method - A Tool for Constrained Global Optimization*, Optimization Methods and Software, **19**, No. 2, (2004), pp. 137–151.

[2] O. Bénichou, R. Voituriez, *Narrow Escape Time Problem: Time Needed for a Particle to Exit a Confining Domain Through a Small Window*, Phys. Rev. Lett, **100**, (2008), 168105.

[3] S. Condamin, O. Bênichou, M. Moreau, *Random Walks and Brownian Motion: A Method of Computation for First-Passage Times and Related Quantities in Confined Geometries*, Phys. Rev. E., **75**, (2007), 021111.

[4] A. Cheviakov, M. J. Ward, *Optimizing the Fundamental Eigenvalue of the Laplacian in a Sphere with Interior Traps*, Mathematical and Computer Modeling, **53**, (2011), pp. 1394–1409.

[5] A. Cheviakov, M. J. Ward, R. Straube, *An Asymptotic Analysis of the Mean First Passage Time for Narrow Escape Problems: Part II: The Sphere*, SIAM J. Multiscale Modeling and Simulation, **8**(3), (2010), pp. 836–870.

[6] D. Holcman, Z. Schuss, *Escape Through a Small Opening: Receptor Trafficking in a Synaptic Membrane*, J. Stat. Phys., **117**, No. 5-6, (2004), pp. 975–1014.

[7] D. Holcman, Z. Schuss, *Diffusion Escape Through a Cluster of Small Absorbing Windows*, J. of Phys. A: Math Theor., **41**, (2008), 155001 (15pp).

[8] GANSO Software Library: University of Ballarat, Ballarat, Victoria, Australia; `www.ballarat.edu.au/ciao`.

[9] M. A. Mammadov, A. Rubinov, J. Yearwood, *Dynamical Systems Described by Relational Elasticities with Applications to Global Optimization*. In: A. Rubinov and V. Jeyakumar (Eds.), *Continuous Optimization: Current Trends and Modern Applications*, Springer, New York, (2005), pp. 365–385.

[10] S. Pillay, M. J. Ward, A. Pierce, T. Kolokolnikov, *An Asymptotic Analysis of the Mean First Passage Time for Narrow Escape Problems: Part I: Two-Dimensional Domains*, SIAM J. Multiscale Modeling and Simulation, **8**(3), (2010), pp. 803–835.

[11] S. Redner, *A Guide to First-Passage Time Processes*, Cambridge Univ. Press, (2001), Cambridge, U.K.

[12] A. Singer, Z. Schuss, D. Holcman, R. S. Eisenberg, *Narrow Escape, Part I*, J. Stat. Phys. **122**, No. 3, (2006), pp. 437–463.

[13] A. Singer, Z. Schuss, D. Holcman, *Narrow Escape, Part II: The Circular Disk*, J. Stat. Phys., **122**(3), (2006), pp. 465–489.

[14] Z. Schuss, A. Singer, D. Holcman, *The Narrow Escape Problem for Diffusion in Cellular Microdomains*, PNAS, **104**(41), (2007), pp. 16098–16103.

[15] A. Singer, Z. Schuss, D. Holcman, *Narrow Escape and Leakage of Brownian Particles*, Phys. Rev. E., **78**, No. 5, (2009), 051111.
[16] G. Szegö, *Ueber Einige Extremalaufgaben der Potential Theorie*, Math. Z., **31**, (1930), p. 583–593.